Technical Physics Letters, 2022, Vol. 48, No. 11

05.1;09.2

Isopachic method with unpolarized light

© V.V. Kesaev

Lebedev Physical Institute, Russian Academy of Sciences, Moscow, Russia
E-mail: vladimir_kesaev@mail.ru

Received September 9, 2022
Revised October 7, 2022
Accepted October 7, 2022

An isopachic method with unpolarized light using a Mach–Zehnder interferometer is proposed. In the case of unpolarized light, isopachics are observed not only due to a change in the thickness of the model but also due to induced birefringence. In contrast to the existing methods, the proposed method allows you to study sections of three-dimensional models or flat stressed samples with no thickness variation. A brief theoretical consideration based on the formalism of the coherence matrix is given, as well as the experimentally obtained isopachic field for a model made from high-modulus material. The method is convenient and simple in technical implementation.

Keywords: photoelasticity, interferometry, stresses, isopachic, isochrome, isocline.

DOI: 10.21883/TPL.2022.11.54898.19360

The photoelastic method is an experimental techniques for analyzing mechanical stresses and provides information on the difference and direction of principal stresses. The main disadvantage of the photoelastic method is the need to separate stresses using additional techniques such as well-known methods: extensometry [1,2], interferometry [3], holographic photoelasticity [4,5], etc. For instance, the authors of [6] proposed isopachics method via analyse of the light intensity patterns for unstressed and solving the transport of intensity equation [7]. Also, an original isopachic method [8] based on the Mach–Zehnder interferometer optical scheme where the signal shoulder being a circular polariscope. The azimuths of an output quarter-wave plate and an analyzer take four discrete values. A numerical analysis of interference patterns provides an opportunity to isolate data on the sum of principal stresses.

We also consider Mach–Zehnder interferometer setup in the present study. The stressed photoelastic model is placed in the signal shoulder (Fig. $1,a$) unpolarized light is fed to the input. A fringe pattern observed at the interferometer output is governed by the Pancharatnam phase [9], which is used to obtain a sum of principal stresses $(\sigma_1+\sigma_2)$.

The coherence matrix formalism [10] provides a convenient way to characterize transmission through the interferometer. The relation between input $\mathbf{M}_0$ and output $\mathbf{M}$ coherence matrices is given by

$$\mathbf{M}=\mathbf{T}\mathbf{M}_0\mathbf{T}^*,\quad \mathbf{T}=\mathbf{T}_s+\mathbf{T}_r, \tag{1}$$

where $\mathbf{M}_0=\mathbf{I}_2$ is a 2×2 unity matrix characterizing unpolarized light and $\mathbf{T}_{s,r}$ are 2×2 transmission matrices for signal and reference interferometer arms. In the reference arm with no model, $\mathbf{T}_r=\mathbf{I}_2$. Transmission matrix $\mathbf{T}_s$ of the signal arm may be written as

$$\mathbf{T}_s=t_1\hat{\mathbf{d}}_1\otimes\hat{\mathbf{d}}_1^*+t_2\hat{\mathbf{d}}_2\otimes\hat{\mathbf{d}}_2^*, \tag{2}$$

where optical axes (eigen vectors) for a plane elastic problem

$$\hat{\mathbf{d}}_1=\hat{\mathbf{x}}\cos\Psi_d+\hat{\mathbf{y}}\sin\Psi_d,\quad \hat{\mathbf{d}}_2=\hat{\mathbf{z}}\times\hat{\mathbf{d}}_1 \tag{3}$$

are related to unit vectors $\hat{\mathbf{x}}$, $\hat{\mathbf{y}}$ of the laboratory reference frame in the model plane via angle Ψ_d (Fig. $1,b$). Two-dimensional distribution $\hat{\mathbf{d}}_{1,2}$ is commonly called the isocline field. The expressions for transmission coefficients $t_{1,2}$ may be approximated as [9]

$$t_{1,2}\approx\exp(i\Phi_{1,2}),\quad \Phi_{1,2}=kn_{1,2}D, \tag{4}$$

where $\Phi_{1,2}$ are absolute phase delays; $n_{1,2}$ are refraction indices for waves polarized linearly in directions $\sigma_{1,2}$; $k=\frac{2\pi}{\lambda}$ is the wave number; λ is the wavelength of used light in vacuum; and D is the geometric thickness of the model.

Let us rewrite expression (1) in an expanded form:

$$\mathbf{M}=\mathbf{M}_r+\mathbf{M}_s+\mathbf{M}_i,\quad \mathbf{M}_i=\mathbf{T}_s\mathbf{M}_0\mathbf{T}_r^*+\mathbf{T}_r\mathbf{M}_0\mathbf{T}_s^*, \tag{5}$$

where $\mathbf{M}_r=\mathbf{T}_r\mathbf{M}_0\mathbf{T}_r^*=\mathbf{M}_0$ is the coherence matrix of the reference beam, $\mathbf{M}_s=\mathbf{T}_s\mathbf{M}_0\mathbf{T}_s^*$ is the coherence matrix of the beam transmitted through the photoelastic model, and $\mathbf{M}_i$ is the interference term. If light at the input is unpolarized and the input matrix is proportional to a unity one ($\mathbf{M}_0=\frac{I_0}{2}\mathbf{I}_2$), output matrix (5) takes the form

$$\frac{\mathbf{M}}{I_0}=\frac{m_0}{2}\mathbf{I}_2+\frac{m_p}{2}\begin{pmatrix}\cos 2\Psi_d & \sin 2\Psi_d\\ \sin 2\Psi_d & -\cos 2\Psi_d\end{pmatrix}, \tag{6}$$

$$\frac{I}{I_0}\equiv m_0=1+\frac{|t_1|^2+|t_2|^2}{2}+\mathrm{Re}\left[e^{-i\Phi_0}(t_1+t_2)\right]$$
$$\approx 2\Big\{1+\cos(\Phi-\Phi_0)\cos(\Delta\Phi)\Big\}, \tag{7}$$

$$m_p=\frac{|t_1|^2-|t_2|^2}{2}+\mathrm{Re}\left[e^{-i\Phi_0}(t_1-t_2)\right]$$
$$\approx -2\sin(\Phi-\Phi_0)\sin(\Delta\Phi), \tag{8}$$

where arguments

$$\Phi = \frac{\Phi_1 + \Phi_2}{2}, \quad \Delta\Phi = \frac{\Phi_1 - \Phi_2}{2} \tag{9}$$

are mean averaged phase shift Φ and phase difference $\Delta\Phi$; Φ_0 is the phase of a wave propagating through the reference interferometer arm; and I_0 is the output light intensity.

The relation between principal stresses and refraction indices (4) for a plane stress state is characterized by Maxwell–Neumann equations

$$n_1 - n_0 = C_1\sigma_1 + C_2\sigma_2, \quad n_2 - n_0 = C_1\sigma_2 + C_2\sigma_1, \tag{10}$$

where C_1, C_2 are optical constants of the model material and n_0 is the refraction index of the unstressed model. Expression (7) for the output intensity is independent of angle Ψ_d and contains data both on isochromes $\Delta\Phi$ and isopachic Φ fields (the locus of points with the same mean phase delay and the same sum of principal stresses). The concept of „visibility“ of fringes

$$V = \frac{I_{\max} - I_{\min}}{I_{\max} + I_{\min}}, \tag{11}$$

where $I_{\max,\min}$ are the maximum and minimum intensities of the interference pattern, is convenient for analysis of the interference pattern. It follows from (7) that, depending on the interferometer adjustment (bright-field or dark-field), isopachics should correspond to maxima or minima of the output intensity pattern. The visibility of these fringes is $V = 1$. The visibility at those points where the phase difference is a multiple of an odd number of half-waves ($\Delta\Phi = \pi\{2N + 1\}$, $N = 0, 1, 2, \dots$) will be zero regardless of the value of mean phase Φ. These points will be isochrome fringes with a half-tone intensity. Figure 2, *a* shows the theoretically calculated example of a moire fringe pattern for a ring that is made of a low-modulus photoelastic material ($C_1 \neq C_2$) and subjected to diametral compression. The pattern is free from isoclines characterized by expressions (3).

If a high-modulus material ($C_1 \approx C_2$), such as mineral or organic glass, is used to fabricate the model, expression (7) takes the form

$$\frac{I}{I_0} \approx 2\{1 + \cos(\Phi - \Phi_0)\}. \tag{12}$$

Only the isopachic field is observed for such materials. Note that both thickness variation $\Delta d = \mu D(\sigma_1 + \sigma_2)/E$ (μ is the Poisson's ratio and E is the modulus of elasticity of the material) and the induced birefringence (see formulae (10)) contribute to mean phase Φ. As a distinct advantage of the proposed method, it is able to analyze stressed models or slices subjected to smoothing and polishing (i.e., with the same thickness). It is indeed sufficient in this case to determine material constants $C_{1,2}$ for calibration models with the surface smoothed after stressing. Figure 2 presents the theoretical and experimental isopachic patterns for an acrylic glass ring subjected to diametral compression.

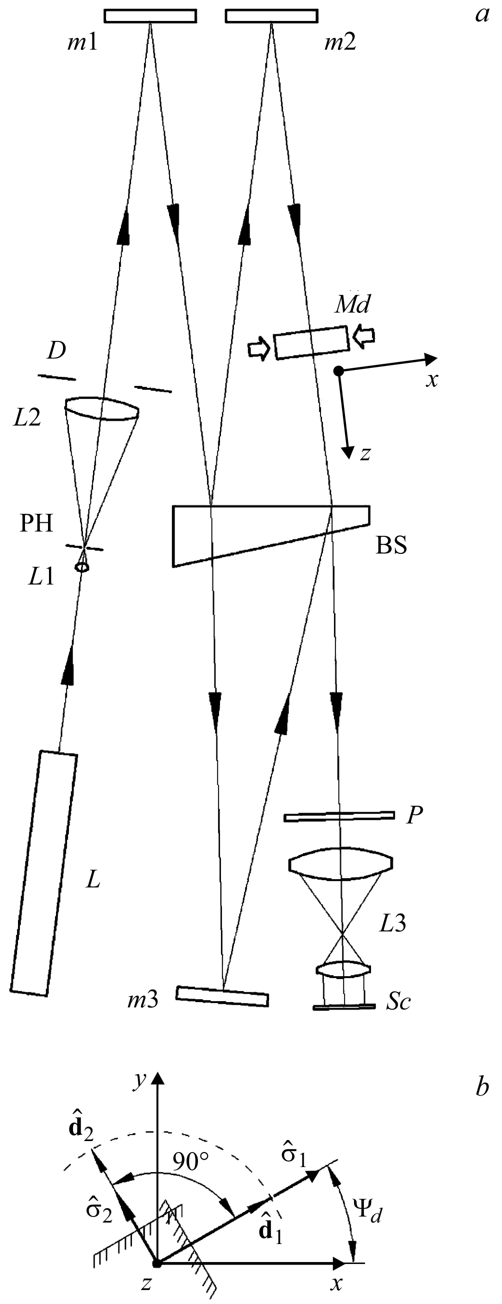

Figure 1. *a* — Mach–Zehnder interferometer used to obtain isopachics. *L* — unpolarized He–Ne laser ($\lambda = 632.8$ nm); *L*1, *L*2 — lenses; PH — pinhole; *D* — aperture; *m* — mirror; *Md* — stressed photoelastic model; BS — beam splitter; *P* — polarizer (optional); *L*3 — telecentric lens; *Sc* — screen. The incidence angles do not exceed 2° so as to suppress the polarizing effect of mirrors. *b* — Directions of vectors $\hat{\mathbf{d}}_{1,2}$ in the laboratory reference frame.

Figure 3, *a* shows the same ring after smoothing and polishing. It can be seen that the fringe value increased (the fringe order decreased).

Unpolarized radiation transmitted through the photoelastic model remains unpolarized and is characterized by a matrix proportional to a unity one. The difference between

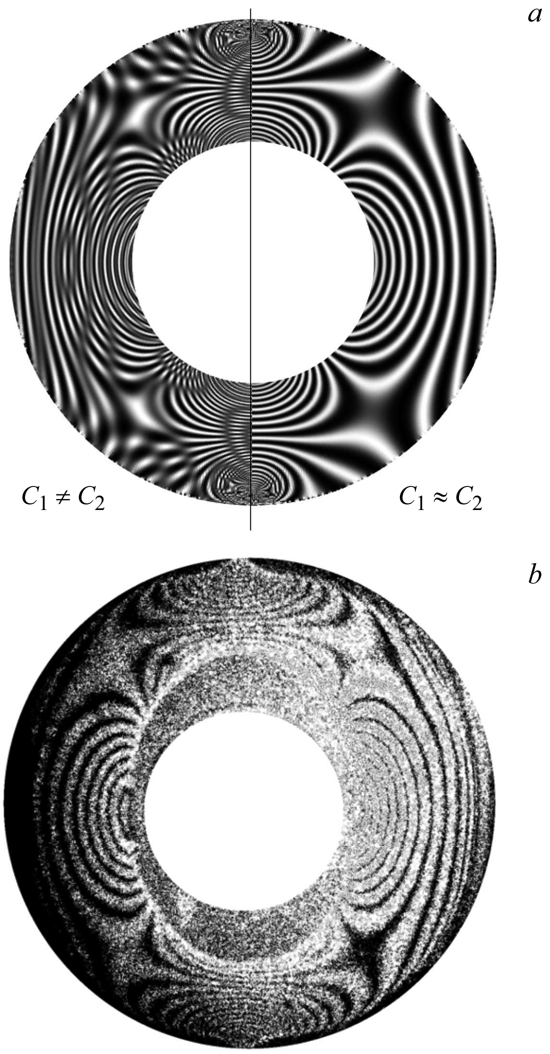

Figure 2. a — Theoretically calculated moire fringe patterns, which are formed by isopachics and isochromes, for a stressed ring made of a low-modulus material with $C_1 = 18.1 \cdot 10^{-11}\,\mathrm{Pa}^{-1}$, $C_2 = 87.6 \cdot 10^{-12}\,\mathrm{Pa}^{-1}$ (left) and a high-modulus material with $C_1 = 60.3 \cdot 10^{-12}\,\mathrm{Pa}^{-1}$, $C_2 = 58.4 \cdot 10^{-12}\,\mathrm{Pa}^{-1}$ (right). The inner and outer radii of the ring are 7.5 and 15 mm, and the thickness is 5 mm. The ring is stressed by a pressure of 39.2 MPa applied at two diametrically positioned 4° sectors. The calculation was performed in accordance with [11]. b — Isopachic pattern for this ring (made from acrylic) observed experimentally in the interferometer. The relative phase difference fell within the $0 < \Delta\Phi \leqslant 8.4^\circ$ range.

output matrix $\mathbf{M}$ and a unity one arises due to interference term $\mathbf{M}_i$ only. Owing to it, two effects are observed at the interferometer output: (1) light intensity modulation specified by formula (7); (2) the output light field is partially polarized with polarization degree

$$P = |m_p|/m_0. \tag{13}$$

Partial polarization, which is induced by the interference of signal and reference beams, gives rise to the dependence of the intensity of light transmitted through a linear polarizer at the interferometer output on polarizer azimuth Ψ_p:

$$I_p(\Psi_p)/I_0 = \left[m_0 + m_p \cos(2\Psi_d - 2\Psi_p)\right]/2. \tag{14}$$

Analyzing this expression, one finds that, depending on $\Delta\Phi$, isopachic fringes may shift by up to π (i.e., an interference maximum is changed to a minimum) when a polarizer is rotated by $\pi/2$. Figure 3, b presents the experimental isopachic patterns for two orthogonal polarizer azimuths (the value of $\Delta\Phi$ remains roughly the same throughout the entire area of the model). It is notable that points retaining their intensity under Ψ_p variations turn out to be isotropic with $P = 0$.

To conclude, we note that the discussed method for stress separation does not require measurements to be performed twice (before and after stressing). In comparison with holographic interferometry techniques, this method offers

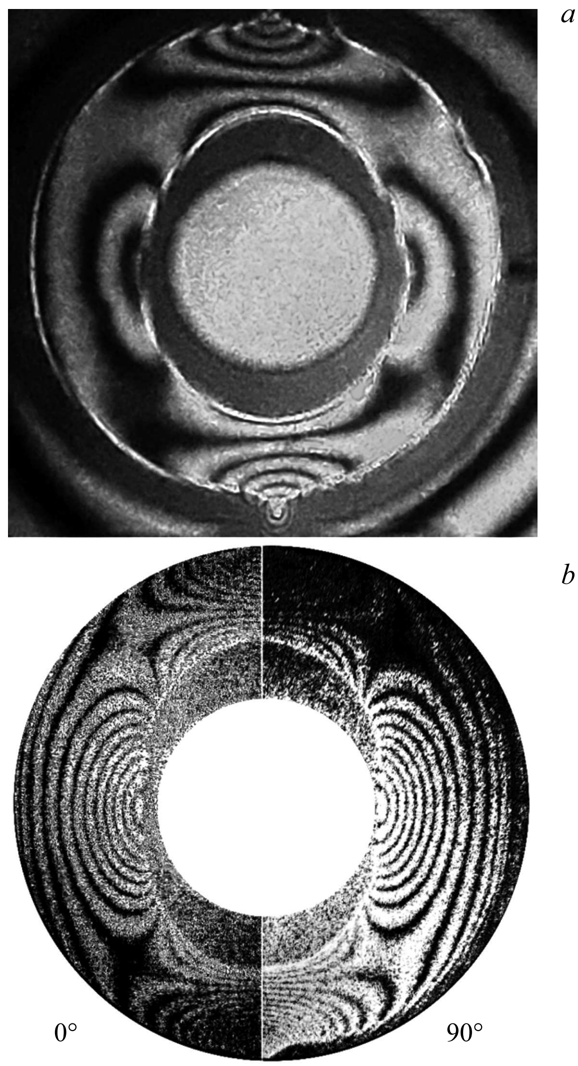

Figure 3. a — Photographic image of isopachics for the ring from Fig. 2 after smoothing and polishing. b — Photographic image of isopachics from Fig. 2, b obtained with a polarizer with azimuth $\Psi_p = 0^\circ$ (left) and 90° (right) mounted at the interferometer output.

an important advantage, as one can examine stresses directly on optically transparent parts and slices with „freeze stresses method“.

Funding

This study was supported by grant No. 20-71-10103 from the Russian Science Foundation.

Conflict of interest

The author declares that he has no conflict of interest.

References

[1] E.G. Coker, L.N.G. Filon, *A treatise on photo-elasticity* (Cambridge University Press, 1931).
[2] M.M. Frocht, *Photoelasticity* (Wiley, N.Y., 1948), vol. 1.
[3] *Metod fotouprugosti*, Ed. by N.A. Strel'chuk, G.L. Khesin (Stroiizdat, M., 1975), Vol. 2, pp. 60–97 (in Russian).
[4] K. Gasvik, Exp. Mech., **16**, 146 (1976). DOI: 10.1007/BF02321109
[5] T. Kihara, H. Kubo, R. Nagata, Appl. Opt., **15**, 3025 (1976). DOI: 10.1364/AO.15.003025
[6] N. Anthony, G. Cadenazzi, H. Kirkwood, E. Huwald, K. Nugent, B. Abbey, Sci. Rep., **6**, 30541 (2016). DOI: 10.1038/srep30541
[7] C. Zuo, J. Li, J. Sun, Y. Fan, J. Zhang, L. Lu, R. Zhang, B. Wang, L. Huang, Q. Chen, Opt. Lasers Eng., **135**, 106187 (2020). DOI: 10.1016/j.optlaseng.2020.106187
[8] H. Yun, Z. Lei, D. Yun, Chin. Opt. Lett., **4**, 164 (2006).
[9] V.V. Kesaev, A.D. Kiselev, E.P. Pozhidaev, Phys. Rev. E, **95**, 032705 (2017). DOI: 10.1103/PhysRevE.95.032705
[10] E.L. O'Neill, *Introduction to statistical optics* (Dover, N.Y., 2003).
[11] Y.V. Tokovyy, K.M. Hung, C.C. Ma, J. Math. Sci., **165**, 342 (2010). DOI: 10.1007/s10958-010-9803-6